THE ASTROPHYSICAL JOURNAL, 470:222–236, 1996 October 10

OBSCURED ACTIVE GALACTIC NUCLEI IN LUMINOUS INFRARED GALAXIES

L. M. SHIER[1]
Naval Research Laboratory, Remote Sensing Division, Code 7217, Washington, D.C. 20375
AND
M. J. RIEKE AND G. H. RIEKE
Steward Observatory, University of Arizona, Tucson, AZ 85721
Received 1996 January 5; accepted 1996 April 30

ABSTRACT

We examine the nature of the central power source in very luminous infrared galaxies. The infrared properties of the galaxies, including their far-infrared and 2.2 μm fluxes, CO indices, and Brackett line fluxes are compared to models of starburst stellar populations. Among seven galaxies we found two dominated by emission from young stars, two dominated by emission from an AGN, and three transition cases. Our results are consistent with evidence for active nuclei in the same galaxies at other wavelengths. Nuclear mass measurements obtained for the galaxies indicate an initial mass function biased toward high-mass stars in two galaxies.

After demonstrating our methods in well-studied galaxies, we define complete samples of high luminosity and ultraluminous galaxies. We find that the space density of embedded and unembedded quasars in the local universe is similar for objects of similar luminosity. If quasars evolve from embedded sources to optically prominent objects, it appears that the lifetime of a quasar is no more than about 10^8 yr.

Subject headings: galaxies: active — galaxies: evolution — galaxies: starburst — galaxies: stellar content — infrared: galaxies — quasars: general

1. INTRODUCTION

The discovery of ultraluminous infrared galaxies immediately raised questions about the relation of these objects to quasars, with which they overlap in luminosity (Rieke & Low 1972). Following their detection in large numbers by *IRAS* (Soifer et al. 1987), this issue has been debated intensely. These galaxies must be in a short evolutionary phase before resuming the appearance of normal spirals and ellipticals. Current theories linking them to active galactic nuclei require that the AGN be present during this infrared luminous phase of evolution (Sanders et al. 1988). However, detecting the AGN can be very difficult given the large amounts of circumnuclear dust. It is even more difficult to determine the role of the AGN in the overall energetics of the galaxy, since the dust degrades the ultraviolet energy into the far-infrared regardless of the energy source. Attempts to determine the roles of star formation and AGNs in these objects have been made more complicated by the subsequent discovery that these objects have both AGNs and circumnuclear starbursts at far above the typical rates. Therefore, the galaxy energetics are often partially derived from each mechanism.

In this paper, we introduce a new approach to solving this dilemma. We construct a five-dimensional space of galaxy properties. Using theoretical starburst models, we locate the small volume in this space that can be occupied by starbursts. We then place the luminous infrared galaxies within this five-dimensional space and determine if they fall within the permitted volume for starbursts, in which case we classify them as starburst dominated. We classify galaxies that fall well away from the starburst domain as AGN dominated.

We test this approach with a sample of seven galaxies, many of which are interacting systems: NGC 1614, NGC 2623, NGC 3690/IC 694, NGC 6240, Arp 220, and Zw 475.056. These galaxies were chosen for their high far-infrared luminosities ($L_{\rm FIR} > 10^{11.4}\ L_\odot$) and low redshifts, and to avoid examples obviously dominated by active nuclei (Mrk 231, for example). We used high-resolution spectroscopy of the 2.3 μm CO bands to measure the nuclear masses and CO indices of these galaxies. Multicolor near-infrared photometry was used to construct extinction corrected absolute K magnitudes. Information on the hot stars came from Brackett line fluxes, and the bolometric luminosities were determined from the *IRAS* data. We find that our classification approach, based on relatively extinction-free observable parameters, is consistent for these well-studied galaxies with all the other indications of the nature of their activity.

Having demonstrated the method, we apply it to two small but complete samples of luminous infrared galaxies. We find from these larger samples that infrared galaxies tend to be strongly starburst dominated up to luminosities of about $10^{11.9}$ $L_\odot$, continuing the trend at lower luminosities. Above this luminosity, there may be a trend to a much larger portion of AGN-dominated objects. The space density of heavily dust embedded quasars is similar to the space density of classical quasars of similar luminosity. This result suggests that the lifetime of quasars is of the order of 10^8 yr or less.

2. OBSERVATIONS

Spectroscopic observations of the CO band-head region were made at the Steward Observatory 2.3 m telescope and at the Multiple Mirror telescope with FSpec, a long-slit near-infrared spectrometer (Williams et al. 1993). Table 1 lists the dates of the observations and the integration times of these observations. In the high-resolution mode, FSpec has a resolving power of $\lambda/\Delta\lambda = 3700 = 80$ km s^{-1} at the 2.3 m and $2500 = 120$ km s^{-1} at the MMT with slits of $2''.4 \times 90''$ and $1'' \times 30''$, respectively.

[1] NRL-NRC Cooperative Research Associate.

TABLE 1

LOG OF SPECTROSCOPIC OBSERVATIONS

Galaxy	Date	Telescope	Time
NGC 1614	1993 Sep 30–Oct 1	SO 2.3 m	4.2[a]
NGC 2623	1994 Mar 29	SO 2.3 m	2.6[a]
NGC 3690	1993 Apr 2	MMT	40[b]
NGC 6240	1993 Mar 31	SO 2.3 m	1.4[a]
IC 694	1993 May 8	SO 2.3 m	2.1[a]
Zw 475.056.....	1993 Sep 30–Oct 1	SO 2.3 m	3[a]

[a] In hours.
[b] In minutes.

Our observational procedures and data reduction are described in Shier, Rieke, & Rieke (1994). The spectra were extracted from a 2".4 × 4".8 aperture except in the case of NGC 3690, where the spectral aperture was 1".0 × 1".2. No attempt was made to flux calibrate the spectra. Spectra for NGC 2623, NGC 3690, NGC 6240, and Zw 475.056 are shown in Figures 1, 2, and 3. Spectra of IC 694 and NGC 1614 may be found in Shier et al. (1994).

Near-infrared images were obtained at the Steward Observatory 2.3 m telescope using a NICMOS3 camera (Rieke et al. 1993b). The filters and plate scales are listed in Table 2. The data were reduced as described by Shier et al. (1994). None of the

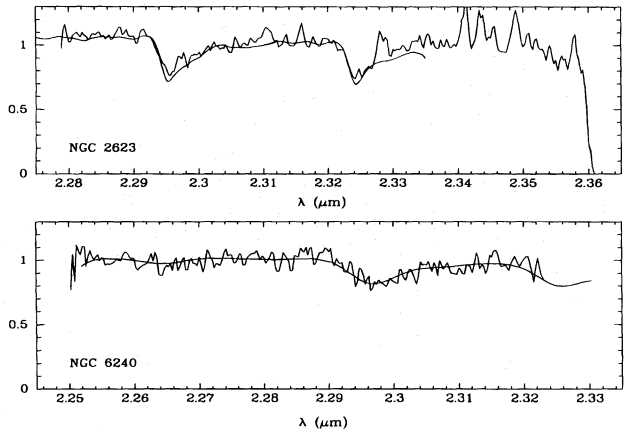

FIG. 1.—The spectra of NGC 2623 and NGC 6240 near the CO (2, 0) band. Also shown is a spectrum of HR 7800 broadened by a Gaussian of width 95 km s^{-1} (NGC 2623) and 360 km s^{-1} (NGC 6240).

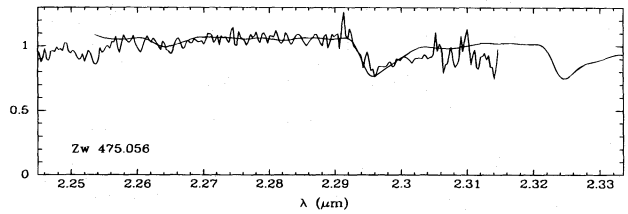

FIG. 2.—The spectrum of Zw 475.046 near the CO (2, 0) band. Also shown is a spectrum of HR 7800 broadened by a Gaussian of width 150 km s^{-1}.

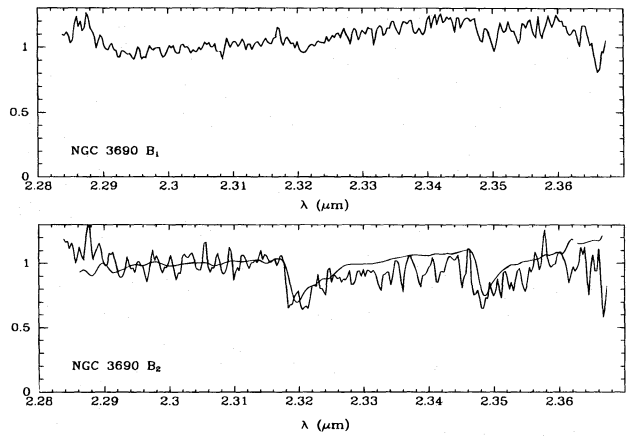

FIG. 3.—The spectra of NGC 3690 B_1 and B_2 near the CO (2, 0) band. Also shown is a spectrum of HR 4299 broadened by a Gaussian of width 66 km s^{-1}.

TABLE 2

LOG OF IMAGING OBSERVATIONS

Galaxy	Date	Filters	Plate Scale[a]
NGC 1614	1992 Nov 4	J, H, K_s	0.6
NGC 2623	1992 Mar 17	J, H, K	0.2
NGC 3690/IC 694.....	1992 Mar 17	J, H, K	0.2
Arp 220.....	1992 Mar 17	J, H, K	0.2
Zw 475.056.....	1992 Nov 4	J, H, K_s	0.6
Zw 475.056.....	1993 Oct 28	K_s	0.2

[a] In arcseconds per pixel.

imaging was done under photometric conditions. Aperture photometry (Carico et al. 1990; Nakagawa et al. 1989) was used to calibrate the images.

3. NUCLEAR PROPERTIES

3.1. *Mass*

The starburst region in a very luminous infrared galaxy is generally less than 1 kpc in size. A brief outline of our procedure for constructing kinematic models of this region to determine its mass was given in Shier et al. (1994); we expand this description below.

3.1.1. *Velocity Dispersion*

We have measured velocity dispersions using the CO (2, 0) near-infrared band at 2.3 μm (Gaffney, Lester, & Telesco 1993; Doyon, Joseph, & Wright 1994a; Shier et al. 1994; Gaffney, Lester, & Doppmann 1995). By measuring in the near-infrared, we minimize complications due to extinction, which is reduced by an order of magnitude compared with the visible. The stars producing the CO band are typically 10^7 or more years old, so at a typical velocity of 100 km s^{-1}, the stars will have moved ~ 1 kpc from their birthsites; i.e., any CO-bearing stars within the starburst region will be well distributed around the nucleus and hence should be good mass probes. In the centers of luminous infrared galaxies, supernovae, gas infall, and massive stellar winds are likely to affect the kinematics of the ionized gas, so the widths of optical and near-infrared emission lines may not be good indicators of the mass of a galaxy. In some merging galaxies, the gas and stars are known to have very different kinematics (Lake & Dressler 1986; Gaffney et al. 1993).

Previous kinematic studies using the CO (2, 0) band (Lester & Gaffney 1994; Doyon et al. 1994b) had very restricted wavelength coverage, requiring specialized approaches for analysis. FSpec in the high-resolution mode has a wavelength coverage of 0.075 μm which allowed us to use the traditional technique of cross-correlation (Tonry & Davis 1979) to determine the velocity dispersion.

Template stars for cross-correlation were chosen to have similar CO band strengths to those of the galaxies and were observed with the identical instrumental parameters as the galaxies. The cross-correlation technique requires that the continuum be subtracted correctly, which is difficult since the true continuum is not seen longward of 2.29 μm because of CO absorption. Traditional methods of continuum fitting proved unsatisfactory when applied to the galaxy spectra. Although it is possible to define a pseudocontinuum in the wing of the CO (2, 0) band, the shape including the pseudocontinuum is not well described by a low-order polynomial. A polynomial of sufficiently high order to match the shape of the pseudocontinuum cannot be fitted to the galaxy spectra due to the noise in the spectra. Removal of low-frequency Fourier components from the spectra is a poor choice for continuum subtraction because the CO bands are sufficiently broad that they contribute power to the low-frequency terms. Therefore, a method was developed based on fitting polynomials to the stellar template spectra that have high signal-to-noise ratios. First, all spectra were divided by the spectrum of HR 7405 (MO III). The quotient spectra are nearly flat and could be fitted with a fourth-order polynomial [excluding the region near the CO (2, 0) band head]. The original spectra were next multiplied by the fit so that their continuum shapes were the same as that of HR 7405. A tenth-order polynomial fit to the spectrum of HR 7405 was then subtracted from each galaxy or template spectrum.

After subtracting the continuum, the galaxies and template stars were cross-correlated in the normal fashion. The uncertainties for the velocity dispersions were obtained from Monte Carlo simulations. The velocity dispersions and uncertainties for each galaxy are listed in Table 3. The velocity dispersion obtained for NGC 6240 is consistent with other values obtained from the CO bands (Doyon et al. 1994b; Lester & Gaffney 1994); the quoted uncertainty is actually a 67% confidence limit. The CO bands in NGC 3690 B_1 are so weak that a reliable velocity dispersion could not be derived. The velocity dispersion listed for Arp 220 is taken from the literature (Doyon et al. 1994) and was obtained with a $2''.2 \times 2''.2$ aperture.

3.1.2. *Kinematic Models*

The relationship between the aperture velocity dispersion and the nuclear mass depends on the kinematic and density structure of a galaxy. It is not obvious whether the CO-bearing stars we measure belong to kinematically hot spherical systems or kinematically cold disk systems. A number of independent lines of reasoning suggest that a kinematically hot model is appropriate for the centers of normal galaxies. However, a disk model may be a better description than a spherical model for the young stars, since they are born in the gas that falls to the center and probably settles into a ring configuration (Barnes & Hernquist 1991). Therefore, the relation between mass and dispersion in our aperture has been calculated for both spherical and disk systems.

Spherical Models.—The velocity dispersion measured from the spectrum is an average of the dispersions in the volume included in the aperture of the spectrograph, weighted by the flux from each volume element. The observed 2.3 μm flux is a

TABLE 3

SPECTROSCOPY RESULTS

Galaxy	Velocity Dispersion (km s^{-1})	Observed CO Index	Corrected CO Index
NGC 1614.....	75 ± 12	0.20 ± 0.01	0.24
NGC 2623.....	95 ± 13	0.145 ± 0.005	0.17
NGC 3690B$_1$.....	...	0.02 ± 0.03	0.04
NGC 3690B$_2$.....	66 ± 33	0.19 ± 0.02	0.19
NGC 6240.....	350 ± 75	0.22 ± 0.02	0.22
IC 694	135 ± 21	0.20 ± 0.02	0.23
Arp 220.....	150 ± 21[a]	0.20 ± 0.05[b]	0.21
Zw 475.056.....	151 ± 28	0.15 ± 0.01	0.17

[a] Doyon et al. 1994b.
[b] Rieke et al. 1985.

function of the density, ρ, mass to 2.3 μm luminosity ratio, γ, and extinction along the line of sight, $e^{-\tau}$. If scattering of light by seeing is neglected, the observed velocity dispersion is given by

$$\sigma_a^2 = \frac{\int_a \sigma_{\rm los}^2(r)\rho/\gamma e^{-\tau}\,dV}{\int_a \rho/\gamma e^{-\tau}\,dV}\,. \tag{1}$$

The integrals in equation (1) are volume integrals that run over the portion of the galaxy seen through the spectroscopic aperture.

The mass density distributions in the spherical models are taken from the analytic η models (Tremaine et al. 1994). These models have central density cusps of variable strength described by the parameter η. We considered the $\eta = 3$ model, in which the density tends to a constant value at small radii, and the $\eta = 2$ model, where $\rho \sim 1/r$ at small radii. To describe the density in physical units, it is necessary to introduce a second parameter, the scale radius, r_s; it is where the density power law changes. The mass interior to a radius r is given by

$$M(r) = \frac{r_s\sigma_a^2}{G}\,\frac{(r/r_s)^\eta}{(1 + r/r_s)^\eta}\,\frac{\int_a \rho/\gamma e^{-\tau}\,dV}{\int_a \bar{v}_{r,\eta}^2(r)\rho/\gamma e^{-\tau}\,dV}\,, \tag{2}$$

where $\bar{v}_{r,\eta}^2(r)$ is the dimensionless velocity dispersion (Tremaine et al. 1994).

In the case of no extinction, and a constant mass-to-light ratio, the mass-aperture dispersion relation of the $\eta = 3$ model reduces to

$$M(r) = \frac{r_s\sigma_a^2}{G}\,\frac{(r/r_s)^3}{(1 + r/r_s)^3}\,\frac{\int_a (1 + 2/r_s)^{-4}\,dV}{\int_a \{[6r/r_s + 1]/[30(1 + r/r_s)^6]\}dV}\,. \tag{3}$$

Disk Models.—If a galaxy has disklike kinematics and structure, then a substantial velocity dispersion will still be measured for the galaxy due to unresolved rotation within the aperture. The observed velocity dispersion is the standard deviation of the velocities of stars within the aperture of the spectrograph. As in the case of the spherical models, the standard deviation is weighted by the flux received from each point within the aperture. The observed velocity dispersion is given by

$$\sigma_a^2 = \frac{\int_a \{[GM(r)]/r\}\cos^2 i \sin^2\theta\rho/\gamma\,dA}{\int_a \rho/\gamma\,dA}\,, \tag{4}$$

where the integrals run over the surface portion of the disk seen in the spectroscopic aperture, θ is the azimuthal coordinate within the galaxy, and i is the inclination of the galaxy.

For a galaxy with a surface mass density given by

$$\Sigma = \Sigma_0\, e^{r/r_e}\,, \tag{5}$$

the mass interior to a radius r is given by

$$M(r) = \frac{r_e\sigma_a^2}{G\cos^2 i}\left[1 - e^{-r/r_e}\left(1 + \frac{r}{r_e}\right)\right]\frac{\int_a \Sigma/\gamma\,dA}{\int_a \{[1 - e^{-r/r_e}(1 + r/r_e)]/r/r_e\}\sin^2\theta\Sigma/\gamma\,dA}\,. \tag{6}$$

3.1.3. *Scale Radii*

The scale radius, r_s, of a spherical model was found by fitting seeing convolved projections of the $\eta = 3$ model density functions to the light profiles. Light profiles were extracted from K or K_s band images (the stars which dominate the CO absorption must also be major contributors to the broadband 2.2 μm light). For most of the galaxies, the light profile was obtained by applying the IRAF ellipse-fitting routine to K or K_s band images. The light profiles of NGC 3690 and Zw 475.056 had to be obtained from major and minor axis cuts due to the double nucleus in NGC 3690, and the unusual light profile of Zw 475.056. The light profile of NGC 6240 was obtained from previously published contour plots (Eales et al. 1990; Zenner & Lenzen 1993). The uncertainty in the scale radii is 0".1–0".2. The scale radii for the spherical models are given in Table 4. The exponential scale radii, r_e, for the disk models were determined by fitting exponentials to the galaxy light profiles; they are

TABLE 4

NUCLEAR MASSES FOR GALAXIES ASSUMING SPHERICAL GEOMETRY

Galaxy	Scale Radius (pc)	Mass $\eta = 3$ ($10^9 M_\odot$)	Mass $\eta = 2$ ($10^9 M_\odot$)
NGC 1614	460	1.5 ± 0.5	1.8 ± 0.6
NGC 2623	340	2.8 ± 0.8	3.0 ± 0.8
NGC 3690 B_1.....	125	...	...
NGC 3690 B_2.....	200	0.6 ± 0.6	0.6 ± 0.6
NGC 6240	620	30 ± 12	41 ± 17
IC 694	220	5.8 ± 1.8	5.8 ± 1.8
Arp 220.....	700	4.6 ± 1.3	6.6 ± 1.3
Zw 475.056.....	600	7 ± 3	5 ± 2

listed in Table 5. The effects of extinction on the scale radii were calculated for a uniform mixture of dust and stars and found to be negligible.

3.1.4. *Calculation of Masses*

The kinematic models in § 3.1.2 were combined with the velocity dispersions and scale radii determined in §§ 3.1.1 and 3.1.3 to estimate the galaxy masses. Except for NGC 3690, the masses are based on a diameter of 1000 pc. This size is appropriate for nuclear starbursts as demonstrated by mid-infrared imaging and photometry (Wynn-Williams et al. 1991; Keto et al. 1992; Wynn-Williams & Becklin 1993), Fabry-Perot imaging (Fischer et al. 1991), and multiaperture spectrophotometry (Joy & Harvey 1987; Moorwood & Oliva 1988; Beck, Turner, & Ho 1990; Doyon et al. 1992). The central region of NGC 3690 has two bright condensations separated by 2".4: B_1 to the south, and B_2 to the north, which were treated independently. The CO band was too shallow to measure the mass of NGC 3690 B_1, and the mass for NGC 3690 B_2 refers to a region with a diameter of 500 pc.

Three models are considered: a spherical model with $\eta = 3$, a spherical model with $\eta = 2$, and a disk model with an inclination of 30° (in a collection of randomly oriented disks, 30° is the median inclination). It is assumed that the mass to 2.2 μm light ratio is constant, and that extinction at 2.2 μm could be neglected. The masses are listed in Tables 4 and 5 along with uncertainties derived from the errors in the velocity dispersions. The effects of extinction and radially dependent mass-to-light ratios were considered, but they were found to cause smaller uncertainties than those from the velocity dispersions. Tables 4 and 5 show that the values for the mass in all three models are also in agreement within the errors imposed by the uncertainties in the velocity dispersions.

3.2. *Absolute K Magnitude*

The 2.2 μm luminosity is an important constraint on the stellar population models described in § 4. The luminosity can be estimated from near-infrared photometry corrected for extinction and the emission by hot dust.

J, H, and K or K_s magnitudes were determined for the central kiloparsec of each galaxy. NGC 3690 B_1 and B_2 were measured separately through 2".4 = 450 pc apertures. Published near-infrared photometry (Thronson et al. 1990) was used to determine the colors and K magnitude of NGC 6240, assuming that the flux-aperture relation is a power law. The K magnitudes and colors of the galaxies are listed in Table 6.

Calculation of the 2.2 μm luminosity of the stars requires that the fraction of the 2.2 μm flux attributable to nonstellar sources be determined. The corrections to the colors and CO indices of the stellar populations in the galaxies were computed under the assumption that the observed fluxes are a mixture of reddened starlight and emission from 750 K dust. A lower limit to the amount of 2.2 μm emission from hot dust was set by requiring that the corrected CO index for the stellar population not exceed 0.24, corresponding to the maximum value in the starburst models described in § 4. The correction for hot dust emission was never permitted to exceed the amount required to place the galaxy on the foreground screen reddening curve for a stellar population. The derived hot dust emission is consistent with the observed $K-L$ colors (Zhou et al. 1993) and 10 μm fluxes (Wynn-Williams & Becklin 1993), assuming that the L and 10 μm fluxes contain emission from dust cooler than the dust that dominates the K-band dust emission.

TABLE 5

NUCLEAR MASSES FOR GALAXIES ASSUMING DISK GEOMETRY

Galaxy	Scale Radius (pc)	Mass ($10^9 M_\odot$)
NGC 1614	300	1.8 ± 0.6
NGC 2623	250	2.9 ± 0.8
NGC 3690 B_1.....	125	...
NGC 3690 B_2.....	200	0.6 ± 0.6
NGC 6240	550	31 ± 12
IC 694	150	5.6 ± 1.8
Arp 220.....	600	4.5 ± 1.2
Zw 475.056.....	700	7 ± 3

TABLE 6

NEAR-INFRARED PHOTOMETRY

Galaxy	Distance (Mpc)	K	$J-H$	$H-K$	Percent Dust[a]	A_V	M_K[b]
NGC 1614	63	10.87	1.14	0.68	15	4.9	−23.5
NGC 2623	74	12.14	1.16	0.67	16	3.8	−22.4
NGC 3690 B_1.....	41	11.83	1.14	1.08	43	3.6	−21.0
NGC 3690 B_2.....	41	11.96	0.88	0.32	0	1.2	−21.3
NGC 6240	97	11.48[c]	1.46[c]	0.52[c]	0	4.4	−24.0
IC 694	41	11.13	1.11	0.68	11	4.6	−22.3
Arp 220.....	73	11.94	1.34	0.71	6	6.4	−23.0
Zw 475.056.....	110	13.30	0.78	0.33	9	0.3	−21.8

[a] Maximum possible contribution of dust to 2.2 μm flux.
[b] Absolute magnitude of stellar component.
[c] See text.

The extinction corrections were calculated both assuming a uniform foreground screen of dust and considering a model with a uniform mixture of dust and stars in a spherical galaxy of the type described in § 3.1.2. The intrinsic colors of the stellar population were taken to be $J-H = 0.75$, $H-K = 0.24$, and $H-K_s = 0.21$; the reddening law was taken from Rieke & Lebofsky (1985). Changes of 0.04 magnitudes in the assumed $H-K$ colors affect the calculated stellar bolometric luminosity by less than 0.1 mag. We found the derived stellar luminosities not to depend strongly on extinction model, because none of the hot-dust–corrected $H-K$ colors implied that the starburst was optically thick at K. We therefore computed the absolute K magnitudes from the hot-dust–corrected $H-K$ color, the foreground screen model, and assuming $H_0 = 75$ km s^{-1} Mpc^{-1}. There remains a possibility of high optical depths that would result in systematic underestimation of the K luminosity (and of other parameters), particularly if the amount of hot dust was smaller than we determined from the CO band depth. Underestimation of the K-band luminosity of our sample galaxies will not affect the conclusions we reach in §§ 4 and 5.

3.3. *CO Index*

A spectroscopic CO index has been defined for red stars and calibrated against the photometric CO index (Kleinmann & Hall 1986). The spectroscopic index samples two regions, one in the continuum shortward of the CO (2, 0) band head at 2.293 μm, and one in the deepest part of the CO (2, 0) band. In applying this method, we applied a correction for velocity dispersion to all of the galaxy CO indices. The photometric CO indices for all the galaxies are presented in Table 3. The CO indices derived here are in agreement with recent measurements from low-resolution spectra (Ridgeway, Wynn-Williams, & Becklin 1994). The CO index after correction for hot dust emission as described in § 3.2 is also listed in Table 3.

3.4. *Ionizing Continuum Luminosity*

The ionizing continuum flux was generally determined from near-infrared hydrogen recombination line fluxes. The extinction to the hot blue stars producing the ionizing continuum may be different than the extinction to the red stars dominating the near-infrared flux, so extinctions to the gas were calculated from the recombination line ratios where possible. We assumed case B intrinsic line ratios (Osterbrock 1989) and took $T_e = 10{,}000$ K in all the galaxies based on studies of IC 694 (Anantharamaiah et al. 1993) and NGC 1614 (Veilleux et al. 1995). The optical/near-infrared extinction law (Rieke & Lebofsky 1985; Cardelli, Clayton, & Mathis 1989) was interpolated to compute A_λ/A_V for each of the hydrogen recombination lines.

For NGC 1614, both Hα/Hβ (Bushouse 1986; Armus, Heckman, & Miley 1989) and Hα/Brγ (Beck et al. 1990) suggest that the extinction to the gas is about $A_V = 3.3$. The Brγ flux in a 5″ aperture and corrected for extinction indicates an ionizing continuum flux of 3×10^{54} photons s^{-1}. This result is consistent with the estimate from Ne II (Roche et al. 1991).

The strong lines of H_2 and the relatively weak hydrogen recombination lines make determination of the ionizing continuum luminosity in NGC 6240 difficult. In low-resolution spectra, Brγ is blended with the 2–1 S (2) line of H_2, a line of comparable strength (Lester, Harvey, & Carr 1988). Using the extinction derived from the near-infrared colors in § 3.2, an upper limit of 4×10^{54} photons s^{-1} to the ionizing continuum luminosity may be obtained from low-resolution, large aperture Brγ flux (Rieke et al. 1985). This estimate is in good agreement with the upper limit to the ionizing continuum derived from the upper limit on the Brα flux (Depoy, Becklin, & Wynn-Williams 1986). A lower limit to the ionizing continuum luminosity of 8×10^{53} photons s^{-1} may be set by considering the high-resolution, small aperture Brγ flux (Lester et al. 1988).

Brγ images of the central region of NGC 3690 (Fischer et al. 1991) suggest that most of the line flux originates in source B_1. The Brα/Brγ ratio (Beck et al. 1986; Fischer et al. 1991) suggests an extinction to the ionized gas of $A_V = 23$. From the Brα flux and the extinction, an ionizing continuum luminosity of 2×10^{54} was computed. In IC 694, Brackett line fluxes in a 7.″2 aperture (Beck et al. 1986) were used to derive an extinction to the ionized gas of $A_V = 16$. The Brα flux, corrected for this amount of extinction, implies an ionizing continuum luminosity of 5×10^{54} photons s^{-1}, in fair agreement with the ionizing continuum flux of 1×10^{54} photons s^{-1} estimated from the H92α line (Anantharamaiah et al. 1993).

The spectrum of NGC 2623 is unusual for a luminous infrared galaxy: Hβ and all of the higher Balmer lines appear in absorption (Armus et al. 1989; Veilleux et al. 1995). By adopting the mean of the two larger aperture Hα fluxes (Keel 1984; Bushouse 1986), and comparing that value to the Brγ flux (Prestwich, Joseph, & Wright 1994), A_V to the line emitting gas can be calculated to be 6.3 (possibly an overestimate, since the observed Hα line flux may be affected by underlying stellar

absorption). The Brγ flux combined with this extinction estimate yields an ionizing continuum luminosity of 1×10^{54} photons s^{-1}; because of the relatively small extinction at Brγ, the uncertainty in intrinsic Hα strength has little effect on this estimate.

The Brα line of Arp 220 has a broad and a narrow component (Depoy, Becklin, & Geballe 1987), suggesting that part of the Brα flux may originate in an active nucleus. The Brγ flux (Rieke et al. 1985; Goldader et al. 1995) is strongly dependent on aperture size, and has never been measured in the same size aperture as Brα (Depoy et al. 1987); only an upper limit of $A_V < 13$ can be calculated from the Brα/Brγ line ratio. The ionizing continuum luminosity of 9×10^{53} photons s^{-1} was computed from the Brα flux in the narrow component, assuming that $A_V = 4.2$, which was determined from the $J-H$ color.

The Brγ flux of Zw 475.056 (Goldader et al. 1995) combined with the A_V computed from the near-infrared J, H, K colors leads to an estimate of 1×10^{54} photon $^{-1}$ for the ionizing continuum.

3.5. *Bolometric Luminosity*

The bolometric luminosity of the very luminous infrared galaxies is nearly equal to their combined mid- and far-infrared luminosity, which can be computed from the *IRAS* measurements (Soifer et al. 1987; Lester & Gaffney 1994). IC 694 and NGC 3690 are in the same *IRAS* beam. Approximately 60% of their combined far-infrared luminosity can be attributed to IC 694 and 40% to the combination of NGC 3690 and Arp 299 C (Joy et al. 1989). Photometry at 25 μm suggests that 10% of the total luminosity of the Arp 299 system originates in source C (Wynn-Williams et al. 1991).

4. ANALYSIS

It is now generally established that highly luminous infrared galaxies tend to harbor active nuclei. AGNs are identified in many of the galaxies in our sample by optical emission-line studies. Armus et al. (1989) find that NGC 2623, Arp 220, and NGC 6240 have LINER-like emission-line ratios, NGC 3690 is an H II region-like galaxy, and NGC 1614 and IC 694 have line ratios that are inconclusive. In another analysis (Veilleux et al. 1995), it was found that NGC 1614 is H II region-like, Arp 220 and Zw 475.056 are Seyfert 2 galaxies, and NGC 6240 is a LINER. Broad Brα emission at 4 μm was found in Arp 220 (Depoy et al. 1987), indicating that this galaxy has a heavily obscured active nucleus.

However, because of the very strong extinction, traditional optical and even near-infrared observations are inadequate to constrain the role of the AGN in the energetics of the galaxy: does it dominate, or is most of the energy due to a starburst with an incidental (energetically) triggering of the AGN? We will address this question systematically in the remainder of this paper. There are three observable properties that have the potential to trace the dominant source of the far-infrared luminosity: (1) hard X-ray emission, which is generally strongly emitted by luminous AGNs; (2) radio emission, which for a starburst will be extended and should be related to the far-infrared luminosity through the radio/FIR relation (Helou, Soifer, & Rowan-Robinson 1985) if this energy is due to star formation; and (3) starburst models. The latter technique is introduced in this paper and is expanded upon below.

In a starburst, it is possible to relate basic properties of the galaxy through an evolutionary model, a technique introduced by Rieke et al. (1980). In the current study, we have determined five relevant properties: mass, 2.2 μm luminosity, CO index, ionizing continuum flux, and bolometric luminosity. We can consider a five-dimensional space in these parameters. For a pure starburst galaxy, only a limited region in this space is accessible; if the galaxy falls significantly out of the permitted region, then an AGN is likely to play an important role in its energetics. Our technique allows the galaxies to be sorted into starburst and AGN dominated groups in a way that is in good agreement with the results from X-ray and radio studies. In § 5, we will analyze two complete samples of these galaxies to determine the space densities of luminous starbursts and of buried AGNs.

4.1. *Stellar Population Models*

We used starburst models developed for M82 (Rieke et al. 1993a). These models include recent treatments of stellar evolution (Maeder 1992). The properties of models with five different star formation rates were considered: a short burst, exponentially declining star formation rates with time constants of 20, 50, and 100 Myr, and constant star formation. All of the models assume that star formation began suddenly, so the values for the observational parameters may not be physically reasonable for model ages less than 5 Myr. Models with star formation rate time constants in excess of 50 Myr have very similar properties, so observationally distinguishing between them is nearly impossible.

Models with two different initial mass functions (IMF), denoted L and S, were compared to the galaxy observations. IMF L is a power-law approximation to the local IMF. IMF S is the initial mass function used to describe the stellar population in M82 (IMF 8 of Rieke et al. 1993a); it is weighted toward high-mass stars, but still retains a significant number of stars of all masses. IMF S is only one example of possible top heavy IMFs; we will also discuss an IMF S', identical to IMF L for masses above 1.5 $M_\odot$ and with no stars below this value. With the exception of the masses, the properties of the IMF L and IMF S models are quite similar, as might be expected because the high-mass parts of the IMFs are similar; the IMF S' models would be identical to IMF L ones for all the timescales of interest, except of course for the smaller mass required. The boundary conditions for the models are listed in Table 7. NGC 3690 is not included because of the uncertainty in the division of bolometric luminosity between source B_1 and source B_2. We illustrate the permitted starburst regions on two-dimensional plots that represent projections of the five-dimensional parameter space in Figures 4 and 5.

The strong CO bands demonstrate that much of the K-band flux from these galaxies is from stars. As shown in Figure 5, the CO index of a stellar population rarely exceeds 0.24. The maximum possible amount of nonstellar emission in the K band is thus found by determining how much nonstellar emission would reduce the CO index from 0.24 to the observed value. The nuclear $K-L$ color and 10 μm flux density place additional constraints on the amount of hot dust emission at K. We have used both the 2.2 μm luminosity and our estimate of the ionizing continuum luminosity to define the most luminous plausible stellar population. In doing so, we ignore the absorption of ionizing continuum by dust in the galaxies, so our estimate of

TABLE 7

NORMALIZED GALAXY PROPERTIES

Galaxy	log (UV) (photons s^{-1})	M_K (mag)	CO Index (mag)	M ($M_\odot$)
NGC 1614	42.9	5.5	0.24	0.004
NGC 2623	42.8	6.3	0.17	0.01
NGC 6240	42.4–43.1	4.7	0.22	0.1
IC 694	43.2	6.5	0.23	0.02
Arp 220	41.8	7.2	0.21	0.004
Zw 475.056.....	42.6	6.7	0.17	0.02

potential hot star luminosity is conservative. When the luminosity of the stellar population is smaller than that of the galaxy, the difference between the total luminosity and the stellar luminosity is assumed to be from the AGN. If the AGN contributes to the hydrogen recombination lines used to calculate the ionizing continuum luminosity, then our procedure would underestimate its luminosity. However, because any AGNs are heavily obscured and hence have weak spectroscopic signatures, and given our conservative approach to estimating the starburst luminosity, we believe the AGN portion of luminosity will be represented roughly correctly.

4.2. *Description of Individual Galaxies*

4.2.1. *NGC 1614*

Stellar population models were found which reproduce satisfactorily the observed properties of NGC 1614. All of the successful models used the M82-based IMF *S*. Models using the local IMF were unable to fit the galaxy parameters within the mass determined by our spectroscopy. Even for the IMF *S* models, the mass-to-light ratio of this galaxy requires that

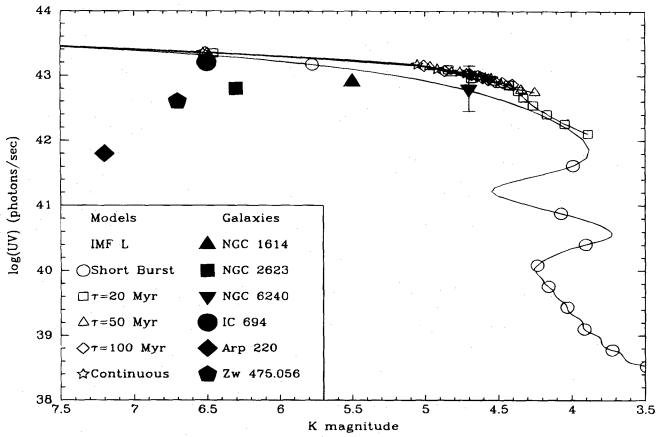

FIG. 4.—Comparison of the ionizing continuum luminosity and 2.2 μm luminosity of the galaxies and the IMF L (solar-neighborhood–like) models. The behavior with the IMF S (M82-like) models is very similar. All luminosities have been normalized to $L_{bol} = 1\ L_\odot$. Models with five star formation rates are shown: a short burst of star formation, lasting 5×10^6 yr, exponentially declining star formation with time constant, τ, equal to 20, 50, or 100 Myr, and a constant star formation rate. Symbols appear every 10 Myr on the model tracks.

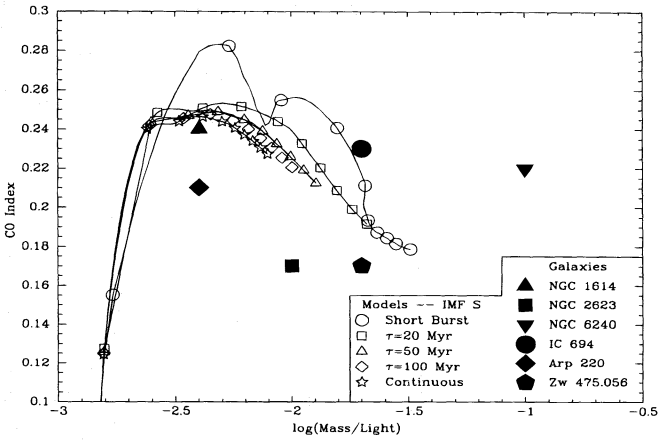

FIG. 5.—Comparison of the CO index and mass-to-light ratio of the galaxies and the IMF S models. The age-CO index relation is similar for the IMF *L* models, but the mass-to-light ratio as a function of age is much higher for the IMF *L* models. Models with five star formation rates are shown: a short burst of star formation, lasting 5×10^6 yr, exponentially declining star formation with time constant, τ, equal to 20, 50, or 100 Myr, and a constant star formation rate. Symbols appear every 10 Myr on the model tracks.

TABLE 8

STARBURST MODEL PROPERTIES

Galaxy	IMF	SFR	Age (Myr)	Mass ($M_\odot$)	Percent Mass in Starburst
NGC 1614	S	Short burst	12	7.4×10^8	49
NGC 6240	L	Short burst	13	2.2×10^9	8
	S	Short burst	13	7.3×10^8	2
	L	$\tau = 100$ Myr	65	6.2×10^9	21
Arp 220.....	L	$\tau = 50$ Myr	73	3.3×10^9	72
NGC 3690 B_1.....	...	Short burst	6	...	...
NGC 3690 B_2.....	S	Short burst	55	3×10^8	50
IC 694	...	...	>15	...	...
NGC 2623	...	...	>10	...	...
Zw 475.056.....	...	...	>10	...	...

the stellar population be less than $\approx$16 Myr old, as shown in Figure 5. Models produce too high an ionizing continuum and too low a 2.2 μm luminosity if they are younger than 11 Myr in the case of a short burst, and 15 Myr for any exponentially declining star formation rate model, as seen in Figure 4. The best-fit stellar population models feature a short burst of star formation that occurred about 12 Myr ago. The details of the best-fitting stellar population for NGC 1614 and the other galaxies are given in Table 8. The properties of the model stellar population are compared to those of NGC 1614 in Figure 6. This figure demonstrates that the stellar population model and the galaxy have similar properties for only a short time. The conclusion that NGC 1614 is starburst-dominated is reinforced by the extent of the radio flux, which gives no indication of a compact nucleus (Condon et al. 1982). No hard X-ray data are available for this galaxy.

Stellar populations with continuing star formation are not allowed by the observations. The conclusion that NGC 1614 has had a very recent burst of star formation is supported by the presence of Wolf-Rayet features (Vacca & Conti 1992), since the ratio of WR/O stars can reach a peak under these conditions that substantially exceeds its maximum value for continuous star formation (Leitherer & Heckman 1995).

The necessity for an M82-like IMF in NGC 1614 is of interest because the extinction in this galaxy is evidently much easier to model than for M82: the levels of obscuration deduced from Hα/Hβ and Brγ/Hα are identical, and the obscuration deduced from the near-infrared stellar colors is similar to that measured from the hydrogen recombination lines. It seems likely that, to first order, the extinction in this galaxy can be described with a foreground screen that is of equal strength for both stars and ionized gas, and the associated level of extinction, $A_V \sim 4$, is modest. Therefore, the complexities of extinction correction that enter in deducing the IMF for M82 seem to be absent for NGC 1614, and the necessity for an M82-like IMF provides an important confirmation of the incidence of top-heavy IMFs in starbursts.

4.2.2. *NGC 6240*

NGC 6240 has the largest 2.2 μm to bolometric luminosity ratio and the largest CO index of all the sample galaxies. Two types of starburst can fit this behavior: (1) a very short burst of star formation about 13 Myr ago; or (2) an exponentially declining star formation rate with time constant of 50 Myr or greater and an age of about 65 Myr. All of the young models have properties that change rapidly, so they fit the properties of NGC 6240 for only a short period. The properties of the older model change slowly, as shown in Figure 7, so a range of ages is possible. In all cases, the starburst uses only a small portion of the dynamical mass, most of which we would attribute to older stars (correction for these stars would move the galaxy to the left in Fig. 5 and onto the starburst locus). In the case of the older models, the IMF L and IMF S' models fit the galaxy better than the IMF S models. The older stellar population model is consistent with the results of earlier stellar population modeling of this galaxy (Rieke et al. 1985). If the ionizing continuum luminosity were better determined in this galaxy, some of the ambiguity about the stellar population could be removed.

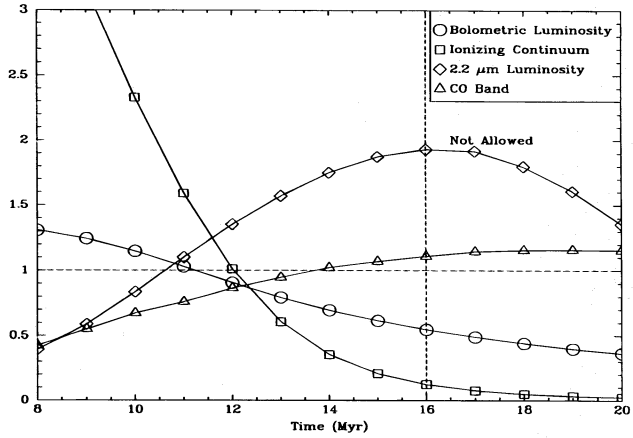

FIG. 6.—The best-fitting model for the stellar population of NGC 1614. This model was created using IMF S and a very short burst of star formation. This model has a mass of $7.4 \times 10^8 M_\odot$. All of the values for the luminosities have been divided by the values observed for the galaxy, so a successful model would have all values equal to one. Note that the region on the right-hand side of the plot is not allowed by the observations because models older than 16 Myr have a mass-to-bolometric luminosity ratio in excess of that observed for the galaxy.

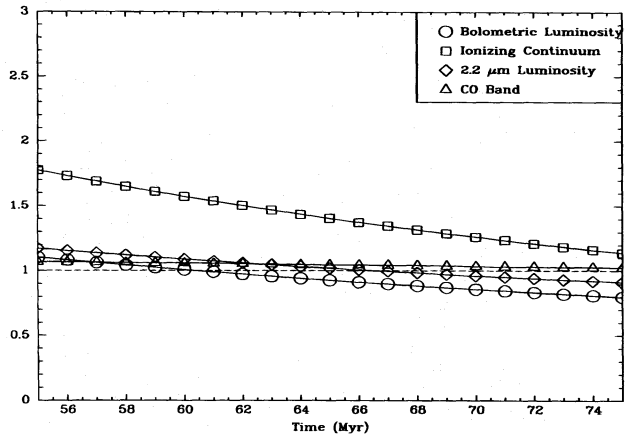

FIG. 7.—A model for the stellar population of NGC 6240. The ionizing continuum flux for the model at 65 Myr is smaller than the upper limit. This model was created using IMF L and a star formation rate that declines exponentially with a time constant of 100 Myr. The model has a mass of $6.2 \times 10^9 M_\odot$. As with Fig. 6, all of the modeled values have been divided by the values observed for the galaxy.

In all cases, less than 25% of the mass in the starburst region need be young stars. It has been suggested that the deep CO bands and relatively high stellar M/L in NGC 6240 present a dilemma for starburst models (Lester & Gaffney 1994). Instead, the galaxy is easily fitted, but it seems likely that at least one of the galaxies in the NGC 6240 merger has contributed a massive population of older stars.

Thronson et al. (1990) have suggested that the far-infrared luminosity of NGC 6240 is predominantly due to dust heated by this old, underlying stellar population. Despite the large mass in these stars, we find that their proposal cannot be correct. The size of the far-infrared source can be determined by comparing ground-based small-aperture photometry with *IRAS* data. Rieke et al. (1985) show that most of the 12 μm flux comes from the inner 6″. A similar test can be made at 25 μm by extrapolating the ground-based photometry to this wavelength using a power-law fit to the *IRAS* 12 and 25 μm data, and correcting to 6″ using the aperture dependence seen at 10.6 μm (data summarized in Rieke et al. 1985). Again, it appears that virtually all the 25 μm flux originates in the inner 6″. We can use our mass determination for the central 1000 pc (=2.″2) and an assumption that the mass scales as the 2.2 μm flux to estimate a mass in this 6″ infrared luminous region of $9 \times 10^{10} M_\odot$. The K flux from an old population of stars of this mass would be 40 mJy (Thronson & Greenhouse 1988), corresponding to a luminosity in these stars of $4.5 \times 10^{10} L_\odot$, only ~10% of the total from this region. That is, the total infrared luminosity is generated almost entirely by a recent starburst. If we deredden the observed m_K by assuming a foreground screen, estimated from the $H-K$ color, we can place a lower limit on the total K flux of twice the estimate of the flux from the old stars. Thus, even the luminosity produced by cool stars must be dominated by the recent starburst.

Our conclusions about NGC 6240 are consistent with the low ratio of hard X-ray to bolometric luminosity (Rieke 1988). They are also in agreement with the radio images of Condon et al. (1982), which show a substantial portion of the radio flux to be extended. NGC 6240 does have a hard X-ray source which was detected by *ASCA* (Nakagawa 1996), but our analysis shows that an active nucleus is not the dominant source of luminosity.

4.2.3. *NGC 3690/IC 694*

We discuss these objects together since they are part of a single system that lies within a single *IRAS* or hard X-ray beam. The 2 μm light of the B_1 source in NGC 3690 appears to be almost entirely nonstellar, as a result of the low CO index of this object. However, a stellar population at an age of 6 Myr and heavily obscured could also produce the observed properties of this object. The source B_2 is dominated by stellar light in the near-infrared, as demonstrated by the strong CO index. The mass to 2.2 μm luminosity ratio of B_2 is also consistent with a starburst. Ages near 50–80 Myr are suggested by the CO index and small observed Brγ flux. Given the age and K magnitude of the starburst, the bolometric luminosity of the starburst in B_2 can be calculated to be about $1 \times 10^{10} L_\odot$. This starburst model, like the one for NGC 1614, requires the use of the M82-like IMF S.

IC 694 lies near the starburst model tracks in Figure 4. However, it can not be fitted by any of the starburst models. The low 2.2 μm to bolometric luminosity and high Brγ flux suggest an age for the stellar population of 10 Myr (7 Myr if all the stars are coeval), but the relatively deep CO band suggests an age of at least 15 Myr (12 Myr for the coeval population). Mixtures of stellar populations of different ages proved equally unsuccessful in reproducing the observed properties of this galaxy. Models of this galaxy that include a starburst and an obscured source show that 65%–90% of the bolometric luminosity of the galaxy must be produced by the obscured source, depending on the age of the starburst, which is not well determined.

Both the stars and active nuclei play an important role in the energetics of this system. Despite the fact that both galaxies in the Arp 299 system may contain active nuclei, at least 20% of the bolometric luminosity of the system must be produced by the combination of the starbursts in IC 694, NGC 3690 B_2, and NGC 3690 C, and up to 60% of the bolometric luminosity of the system as a whole may produced by stars, if source B_1 is a very young starburst.

4.2.4. *NGC 2623*

From the CO strength, stars contribute about 85% of the K-band light. A stellar population like that in NGC 1614 is permitted for this galaxy. Such a population would produce 85% of the 2.2 μm luminosity, 40% of the bolometric luminosity, and all of the observed Brγ flux. A combination of an AGN and a stellar population model older than 10 Myr is permitted by

the observations if a large fraction of the Brγ flux is produced by the AGN. These arguments imply that about half of the luminosity is from an AGN.

The strong Balmer absorption lines in NGC 2623 suggest that a substantial intermediate age (about 1 Gyr) stellar population is present in this galaxy (Armus et al. 1989). However, some of the stars in this galaxy are clearly young. The 2.2 μm stellar luminosity-to-mass ratio will not permit single age stellar populations older than 300 Myr.

The radio image of NGC 2623 is well resolved (Condon et al. 1991), contrary to expectations for an AGN-dominated galaxy and possibly the result of the complex star forming history discussed above. A radio core having a brightness temperature exceeding 10^7 K is detected with VLBI (Lonsdale, Smith, & Londsdale 1993). The data are consistent with the presence of a point source within a complex structure. This galaxy is therefore an ambiguous case, with evidence for substantial roles for both an AGN and star formation in its energetics.

4.2.5. *Arp 220*

There are no stellar population models that can fit all of the properties of Arp 220. The 2.2 μm to bolometric luminosity ratio is inconsistent with any of the stellar population models with ages over 10 Myr. Neither the CO index nor the ionizing continuum luminosity permit such a young age for the stellar population. However, if the reddening at K is underestimated substantially (2.5 mag), then the properties become consistent with the starburst models. In this case, however, the restrictions on the IMF become extreme.

The strong CO bands in Arp 220 require that at least 90% of the observed 2.3 μm flux of this galaxy be generated by stars. If the nonstellar emission at 2.3 μm is from hot dust, then dust can provide no more than 6% of the total K-band luminosity. If it is assumed that a hidden active nucleus is contributing to the bolometric luminosity, but not the 2.2 μm luminosity or the narrow Brα flux, then it is possible to find a stellar population model for this galaxy that produces about 8% of the bolometric luminosity. It has an exponentially declining star formation rate with a time constant of 50 Myr and an age of 73 Myr. The IMF L model (or the IMF S' model) is a better fit than the IMF S model, and it would require 72% of the total mass to be in the form of young stars, just to produce 8% of the observed bolometric luminosity. Being mindful of the reddening uncertainties, a young stellar population with IMF S' or IMF S might produce up to 30%–40% of the bolometric luminosity, but it appears that Arp 220 must generate a substantial portion of its luminosity from an AGN unless the IMF for recent star formation in this galaxy is exceedingly biased toward massive stars.

A radio core is detected with VLBI in Arp 220 (Lonsdale et al. 1993), but the structure is not consistent with a single high brightness temperature source. The galaxy is undetected in hard X-rays (Rieke 1988); if it harbors a powerful AGN, this object must be hidden by extreme interstellar absorption along our line of sight. Taken together, we have to conclude that this galaxy appears to have significant portions of its energy generated by both young stars and by an AGN, but that the extinction is sufficiently great to make more detailed determinations difficult.

4.2.6. *Zw 475.056*

The ratio of 2.2 μm to bolometric luminosity is inconsistent with all the luminosity being produced by any stellar population more than 10 Myr old, and the ionizing continuum flux and CO index are inconsistent with such a young stellar population.

Many models in which an AGN is combined with a stellar population are consistent with the observed properties of Zw 475.056. It is not possible to determine the exact nature of the stellar population, but some limits may be placed on its properties. If the stellar population has a CO index near 0.24, which is typical of the younger starburst models, then the stars produce about two-thirds of the observed 2.3 μm flux. A stellar population like that observed in NGC 1614 is allowed for this galaxy and would produce 25% of the bolometric luminosity. Older models require that some of the observed Brγ flux be produced by the active nucleus. In all cases, the AGN plays an important role in producing the galaxy luminosity.

The radio image of Zw 475.056 is dominated by a compact source (Condon et al. 1991), as expected. However, no VLBI core was found in this galaxy (Lonsdale et al. 1993).

4.3. *Summary*

We find that the types of nuclear activity in galaxies deduced from stellar population modeling are consistent with other data in a sample of seven well-studied luminous infrared galaxies. Within this sample, we find that two are starburst dominated, two are probably AGN dominated, and three are transitional cases.

For one of the starburst-dominated galaxies, NGC 1614, and one of the starburst nuclei in a transitional case, NGC 3690 B_2, the IMF appears to be biased toward high-mass stars, as was found previously for M82 (Rieke et al. 1993a). These galaxies are important examples of this phenomenon because their starbursts appear to be relatively lightly obscured, reducing the uncertainties in the determination of their intrinsic properties compared to M82.

Assuming such an IMF is appropriate in other cases, we find that sufficient mass is available in all the luminous galaxies to account for the levels of star formation indicated by other parameters. In most cases, even a local-type IMF suffices to support this statement. There is still uncertainty about how to apportion the dynamical mass among young stars, old stars, and gas (Shier et al. 1994). However, only in the extreme case of Arp 220 is the value of M/L so low that it suggests that an AGN is required to power the galaxy.

5. SPACE DENSITY OF BURIED AGNS AND AGN LIFETIMES

It is not technically feasible to obtain an accurate 2.3 μm CO-based mass for most ultraluminous galaxies. However, the results of the preceding section suggest we can model these objects under the assumption that they will have sufficient mass to sustain nuclear starbursts if such events are indicated by other observable parameters. We therefore have defined two

complete samples of such galaxies for which only low-resolution infrared spectroscopy is generally available. The samples are listed in Tables 9 and 10. The high-luminosity sample consists of galaxies with $10^{11.3}\ L_\odot < L < 10^{11.9}\ L_\odot$, while the ultraluminous sample contains galaxies with $L > 10^{11.9}\ L_\odot$. In addition to the luminosity limits, sample members are required to lie north of 30° declination. We have tested the samples for completeness with the V/V_{max} test (Schmidt 1968). The 13 high-luminosity galaxies within 100 Mpc ($H_0 = 75$ km s^{-1} Mpc^{-1}) have $\langle V/V_{max}\rangle = 0.53$, while the seven ultraluminous galaxies within 200 Mpc have $\langle V/V_{max}\rangle = 0.49$, indicating both samples are reasonably complete.

We model these galaxies in a manner similar to that introduced in § 4 to determine the role starbursts play in their energetics. It has been suggested that ultraluminous galaxies frequently harbor dust-enshrouded quasars and that such hidden objects may even dominate the local space density of quasars. Such hypotheses can be tested by the arguments below.

5.1. *Optical Depths*

Before proceeding with the analysis of these samples, we note that Goldader et al. (1995) have compared the trends of Brγ and FIR luminosity and conclude that an abrupt change occurs at the boundary between high and ultraluminous galaxies, in that the ultraluminous galaxies "are, as a group, deficient in Brγ photons relative to less luminous infrared galaxies." They further argue that the implied huge 2 μm optical depths make the energy sources of the ultraluminous galaxies uniquely difficult to determine. We agree with Goldader et al. (1995) that optical depth effects are important in the ultraluminous galaxies, but we see them as an increasing trend rather than a sudden transition and hence believe that these galaxies can be treated in a consistent manner with the lower luminosity ones. To support our view, we illustrate in Figure 8 the relation between Brγ and far-infrared luminosity over a much wider luminosity range than they examined. We find that the best-fitting slope (in a least-squares sense) is 0.68 ± 0.05. If the galaxies are optically thick in Brγ and optically thin in the far-infrared, then the expected slope is given by the ratio of surface area to volume, which for a simple solid is 0.67. A variety of other geometric models would give similar behavior. The good agreement with the observations suggests that this naive model is correct to first order, and that a smooth progression toward higher optical depths occurs with increasing luminosity beginning with even relatively low luminosity infrared galaxies. The evidence for a sharp transition at $10^{12}\ L_\odot$ in the data of Goldader et al. (1995) seems to arise from their fitting a slope of 1.33 to the high-luminosity galaxies alone, probably due to an inadequate baseline in luminosity. This anomalously high slope gives the appearance of a break when the normal relation is recovered at even higher luminosities.

5.2. *Space Density of Types of Luminous Galaxies*

Given that optical depth effects are likely to be pervasive in both of our luminous galaxy samples, we have analyzed their possible energy sources in the following manner. We have placed them in the five-dimensional parameter space discussed in § 4, based on the best estimates of their properties with correction for extinction. In general, these estimates have assumed a foreground screen of dust and hence are both oversimplified and biased toward underestimating the extinction. Hence, if these galaxies could be placed on a permitted starburst locus in the parameter space by a consistent increase in the reddening correction for all parameters, we count them as galaxies that are potentially predominantly powered by starbursts.

TABLE 9

HIGH-LUMINOSITY SAMPLE

Galaxy	V_{rec} (km s^{-1})	log L_{IR} ($L_\odot$)	Type
NGC 34	5931	11.3	SB
IC 1623	5550	11.4	SB
NGC 1614	4745	11.6	SB
UGC 3608	6488	11.3	SB
NGC 2623	5538	11.6	SB/AGN
NGC 3690/IC 694	3115	11.6	SB/AGN
Arp 193	6870	11.6	SB
NGC 5257/8	6820	11.4	SB
IRAS 16164−0746	6674	11.4	...
MCG +01-42−088	7075	11.3	SB
NGC 6240	7393	11.8	SB
IRAS 17138−1017	5323	11.4	SB
NGC 7469	4963	11.6	SB/AGN

TABLE 10

ULTRALUMINOUS SAMPLE

Galaxy	V_{rec} (km s^{-1})	log L_{IR} ($L_\odot$)	Type
IRAS 05189−2524	12706	12.1	AGN
UGC 5101	12000	11.9	SB/AGN
IRAS 10565+2448	12501	12.0	SB
Mrk 231	12556	12.5	AGN
Mrk 273	11400	12.1	SB
Arp 220	5452	12.2	SB/AGN
IRAS 17208−0014	12946	12.4	SB

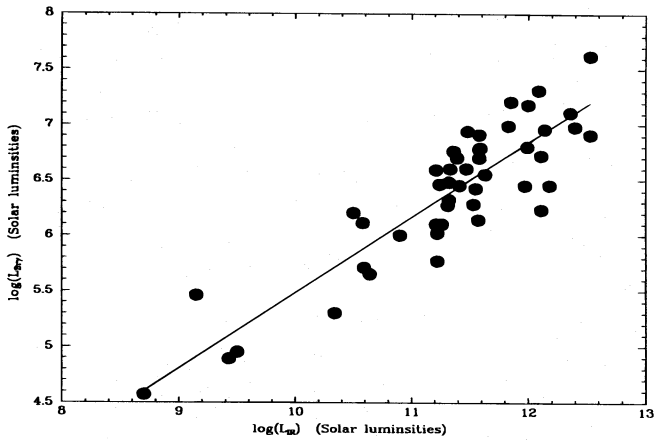

FIG. 8.—Comparison of L_{bol} and $L_{Br\gamma}$ for infrared galaxies. Data are from the literature and unpublished observations. Galaxies plotted include those from Goldader et al. (1995), and starburst and composite systems that are primarily starburst from Moorwood & Oliva (1988) (i.e., II Zw 40, M82, NGC 6946, NGC 253, etc.). The line is a best fit through all the data points; it has a slope of 0.68 ± 0.05.

The conditions for starburst power are still quite restrictive. The addition of an AGN simply adds free parameters to fit the galaxy properties without the constraints of the laws of stellar evolution. By Occam's Razor, if the galaxy can be powered by a starburst we assume that it is in fact powered in this manner.

Three galaxies in the high-luminosity sample (NGC 34, IC 1623, and NGC 5257/8) have no infrared spectroscopy in the literature; we classify them as starbursts on the basis of their extended radio sources (Condon et al. 1991). In support of this classification, the latter two are also very extended at 10 μm (Carico et al. 1988), requiring them to have an extended luminosity source powering their infrared emission. We then find of the 13 high-luminosity galaxies, nine are starburst dominated, one is ambiguous because of lack of data (IRAS 16164−0746), one is a well-known composite AGN/SB system (NGC 7469), and two more (NGC 2623 and NGC 3690/IC 694) have indications of embedded AGNs that might account for up to ~50% of their outputs. For the ultraluminous galaxies, we find that three are starburst dominated (IRAS 10565+2448, Mrk 273, and IRAS 17208−0014) and the remaining four are AGN dominated or have a strong AGN component.

Various studies (e.g., Soifer et al. 1987) have shown that the portion of infrared galaxies with AGNs increases as the luminosity increases. Our samples illustrate that the AGN is in general not energetically dominant until the ultraluminous stage is reached. Up to $L \sim 10^{11.9}\ L_\odot$, it appears that the energetics of most infrared galaxies are dominated by star formation.

From the initial discovery of ultraluminous infrared galaxies (Rieke & Low 1972), their relation to quasars has been a matter for active speculation. In our high-luminosity sample, we find only three objects with potentially strong AGNs. Since the classic Seyfert galaxy NGC 7469 is of type 1, its nuclear region cannot be embedded. Two other galaxies (NGC 3690/IC 694 and NGC 2623) possibly have moderate luminosity ($\sim 10^{11.3}\ L_\odot$) embedded AGNs that fall in the Seyfert luminosity range. A fourth, IRAS 16164−0746, has insufficient data for classification. We can estimate the space density of embedded AGNs in this luminosity range by multiplying the appropriate space density for all *IRAS* sources (e.g., Rieke & Lebofsky 1986; Soifer et al. 1987) by the appropriate fraction. We find a value of roughly 4×10^{-7} Mpc^{-3} mag^{-1} for dust-embedded high-luminosity Seyfert nuclei. In our ultraluminous sample, we find two objects that are clearly AGN-dominated (IRAS 05189−2524 and Mrk 231) and two additional objects that are probably AGN-dominated (UGC 5101 and Arp 220). The same procedure suggests a space density of $\sim 4 \times 10^{-8}$ Mpc^{-3} for embedded AGNs of luminosity greater than $10^{11.9}\ L_\odot$.

Using the spectral energy distributions obtained by Edelson & Malkan (1986), we estimate that an embedded low-luminosity quasar ($-23 > M_B > -24.1$) would emit in the range of $L_{FIR} = 10^{11.5}$–$10^{11.9}\ L_\odot$ or higher. Similarly, an embedded high-luminosity quasar ($-24.1 > M_B$) would have $L_{FIR} > 10^{11.9}\ L_\odot$ or more. We estimate the space density of low-luminosity quasars from Schmidt & Green (1983) to be 8×10^{-8} Mpc^{-3}. Similarly, for high-luminosity quasars we find a density of 1.6×10^{-8} Mpc^{-3}. We estimate the space density of Seyfert galaxies with $10^{11.0}\ L_\odot < L < 10^{11.5}\ L_\odot$ to be roughly 10^{-6} Mpc^{-3} from Huchra & Burg (1992). The estimates for low-luminosity quasars and for Seyfert galaxies are likely to be low by a factor of 2 or more due to the bias against finding such nuclei in edge-on galaxies. Within the errors, the values for quasars are closely comparable with the values for embedded quasars of similar luminosity. That is, within the local volume of space, it appears that the numbers of embedded and unembedded quasars are similar. The space density of embedded Seyfert nuclei appears to be significantly lower than for unembedded nuclei of similar luminosity.

5.3. *AGN Lifetimes*

Among the four embedded ultraluminous AGNs discussed above, at least two appear to have accompanying circumnuclear starbursts. We have already discussed the case of Arp 220 at length. In addition, UGC 5101 shows a strong extended radio source surrounding its compact core (Condon et al. 1991) and appears to be extended at 10 μm. It has been suggested that a third of these objects, Mrk 231, is also undergoing a starburst (e.g., Solomon, Downes, & Radford 1992; Lipari, Colina, & Macchetto 1994; Smith et al. 1995).

Starbursts impose a natural clearing time on the nuclear interstellar medium of a galaxy, as huge amounts of mechanical energy are released due to stellar winds and supernova explosions (Rieke et al. 1980; Fabbiano 1988; Tomisaka & Ikeuchi

1988). The episode of supernova explosions ends roughly 30 Myr after the formation of massive stars (Leitherer & Heckman 1995), and in general it appears that the ISM is cleared on a timescale of this order.

We can use the clearing timescale of the nuclear ISM by circumnuclear starbursts to limit the lifetimes of AGNs. We assume that the AGNs embedded in the ultraluminous infrared galaxies are intrinsically the same as those seen in unembedded cases. We are left with two possibilities. The first is that the luminosities of these AGNs decay substantially during the ISM clearing time, so that we identify their older counterparts as Seyfert nuclei. This hypothesis would set a limit of approximately 30–50 Myr on the lifetime of an AGN before it fades substantially. The second possibility is that the embedded AGNs maintain similar energy levels until after they are revealed, in which case we would identify them as quasars. In this case, since we see roughly equal space densities of embedded AGNs and quasars, we estimate the AGN lifetime to be roughly twice as long, 60–100 Myr, after which the source must fade quickly. Applying similar arguments, our data suggest that luminous Seyfert nuclei have significantly longer lifetimes than do quasars.

6. CONCLUSIONS

We have examined in detail the power sources for seven very luminous galaxies. We determined the masses of each nucleus from the stellar velocity dispersion as measured with the relatively extinction-free first overtone CO bands at 2.3 μm. We also determined the bolometric luminosities, CO indices, absolute K magnitudes, and ionizing continuum luminosities for these galaxies. We use these data to test a technique based on starburst modeling to examine whether these galaxies are starburst or AGN dominated. We find:

1. Modeling these five starburst parameters gives results consistent with the other indicators of the dominant luminosity sources for these galaxies, and the results would generally be unchanged with models based only on the four parameters of bolometric and ionizing continuum luminosity, CO index, and absolute K magnitude.
2. In two cases (NGC 1614 and NGC 3690 B_2) there is strong evidence for the starburst IMF being top heavy compared with that in the solar neighborhood.
3. Contrary to previous suggestions (Lester & Gaffney 1994), the large dynamical mass of NGC 6240 posed no problem for starburst models; on the other hand, this mass is insufficient to allow the luminosity of this galaxy to be produced by old stars, as had been suggested by Thronson et al. (1990).

Based on these results, we have applied the starburst modeling technique to two complete samples of galaxies, many of which have not been studied in the same detail as the seven test galaxies discussed above. We find from these complete samples:

1. Most infrared galaxies with luminosities below $10^{11.9}\ L_\odot$ are strongly starburst dominated.
2. The portion of AGN-dominated systems may increase significantly above $10^{11.9}\ L_\odot$.
3. The space density of embedded quasars is similar to the space density of unembedded quasars of similar luminosity.
4. From conclusion 3 and the timescale for star formation to clear the interstellar medium around a galactic nucleus, it appears that the lifetime of a quasar is no more than 10^8 yr.

Thanks are due to Hans-Walter Rix for tips on kinematic modeling, and to John Black for discussion on a variety of topics. Funding for the instrumentation used in this project came from NASA (NICMOS3 array development), NSF (general funding for FSpec), and Zonta International, an association of professional women (FSpec's high-resolution diffraction grating). NASA, through the Graduate Student Researchers Program, provided support for L. M. S.

REFERENCES

Anantharamaiah, K. R., Zhao, J.-H., Goss, W. M., & Viallefond, F. 1993, ApJ, 419, 585
Armus, L., Heckman, T. L., & Miley, G. K. 1989, ApJ, 347, 727
Barnes, J. E., & Hernquist, L. E. 1991, ApJ, 370, L65
Beck, S. C., Turner, J. L., & Ho, P. T. P. 1986, ApJ, 309, 70
———. 1990, ApJ, 359, 57
Bushouse, H. A. 1986, AJ, 91, 255
Cardelli, J. M., Clayton, G. C., & Mathis, J. S. 1989, ApJ, 345, 245
Carico, D. P., Sanders, D. B., Soifer, B. T., Elias, J. H., Matthews, K., & Neugebauer, G. 1988, AJ, 95, 356
Carico, D. P., Sanders, D. B., Soifer, B. T., Matthews, K., & Neugebauer, G. 1990, AJ, 100, 70
Condon, J. J., Condon, M. A., Gisler, G., & Pushell, J. J. 1982, ApJ, 252, 102
Condon, J. J., Huang, Z. P., Yin, Q. F., & Thuan, T. X. 1991, ApJ, 378, 65
Depoy, D. L., Becklin, E. E., & Geballe, T. R. 1987, ApJ, 315, L63
Depoy, D. L., Becklin, E. E., & Wynn-Williams, C. G. 1986, ApJ, 307, 116
Doyon, R., Joseph, R. D., & Wright, G. S. 1994a, ApJ, 421, 101
Doyon, R., Puxley, P. J., & Joseph, R. D. 1992, ApJ, 397, 117
Doyon, R., Wells, M., Wright, G. S., Joseph, R. D., Nadeau, D., & James, P. A. 1994b, ApJ, 437, L23
Eales, S. A., Becklin, E. E., Hodapp, K.-W., Simons, D. A., & Wynn-Williams, C. G. 1990, ApJ, 365, 478
Edelson, R. A., & Malkan, M. A. 1986, ApJ, 308, 59
Fabbiano, G. 1988, ApJ, 330, 672
Fischer, J., Smith, H. A., & Glaccum, W. 1991, in ASP Conf. Ser., Vol. 14, Astrophysics with Infrared Arrays, ed. R. Elston (San Francisco: ASP), 63
Gaffney, N. I., Lester, D. F., & Doppmann, G. 1995, PASP, 107, 68
Gaffney, N. I., Lester, D. E., & Telesco, C. M. 1993 ApJ, 407, L57
Goldader, J. D., Joseph, R. D., Doyon, R., & Sanders, D. B. 1995, ApJ, 444, 97
Helou, G., Soifer, B. T., & Rowan-Robinson, M. 1985, ApJ, 298, L7
Huchra, J., & Berg, R. 1992, ApJ, 393, 90
Joy, M., & Harvey, P. M. 1987, ApJ, 315, 480
Joy, M., Lester, D. F., Harvey, P. M., Telesco, C. M., Decher, R., Rickard, L. J., & Bushouse, H. 1989, ApJ, 339, 100
Keel, W. C. 1984, ApJ, 282, 75
Keto, E., Ball, R., Arens, J., Jernigan, G., & Meixner, M. 1992, ApJ, 387, L17
Kleinmann, S. G., & Hall, D. N. B. 1986, ApJS, 62, 501
Lake, G., & Dressler, A. 1986, ApJ, 310, 605
Leitherer, C., & Heckman, T. M. 1995, ApJS, 96, 9
Lester, D. F., & Gaffney, N. I. 1994, ApJ, 413, L13
Lester, D. F., Harvey, P. M., & Carr, J. 1988, ApJ, 329, 641
Lipari, S., Colina, L., & Macchetto, F. 1994, ApJ, 427, 174
Lonsdale, C. J., Smith, H. E., & Lonsdale, C. J. 1993, ApJ, 405, L9
Maeder, A. 1992, private communication
Moorwood, A. F. M., & Oliva, E. 1988, A&A, 203, 278
Nakagawa, T. 1996, private communication
Nakagawa, T., Nagata, T., Geballe, T. R., Okuda, H., Shibai, H., & Matsuhara, H. 1989, ApJ, 340, 729
Osterbrock, D. E. 1989, Astrophysics of Gaseous Nebulae and Active Galactic Nuclei (Mill Valley, CA: University Science Books)
Prestwich, A. H., Joseph, R. D., & Wright, G. S. 1994, ApJ, 422, 73
Ridgway, S. E., Wynn-Williams, C. G., & Becklin, E. E. 1994, ApJ, 428, 609

Rieke, G. H. 1988, ApJ, 331, L5
Rieke, G. H., Cutri, R. M., Black, J. H., Kailey, W. F., McAlary, C. W., Lebofsky, M. J., & Elston, R. 1985, ApJ, 290, 116
Rieke, G. H., & Lebofsky, M. J. 1985, ApJ, 288, 618
———. 1986, ApJ, 304, 326
Rieke, G. H., Lebofsky, M. J., Thomson, R. I., Low, F. J., & Tokunaga, A. T. 1980, ApJ, 238, 24
Rieke, G. H., Loken, K., Rieke, M. J., & Tamblyn, P. 1993a, ApJ, 412, 99
Rieke, G. H., & Low, F. J. 1972, ApJ, 176, L95
Rieke, M. J., Rieke, G. H., Green, E. M., Montgomery, E. F., & Thomson, C. L. 1993b, Proc. SPIE, 1946, 179
Roche, P. F., Aitkin, D. K., Smith, C. H., & Ward, M. J. 1991, MNRAS, 248, 606
Sanders, D. B., Soifer, B. T., Elias, H. J., Madore, B. F., Matthews, K., Neugebauer, G., & Scoville, N. Z. 1988, ApJ, 325, 74
Schmidt, M. 1968, ApJ, 151, 393
Schmidt, M., & Green, R. F. 1983, ApJ, 269, 355
Shier, L. M., Rieke M. J., & Rieke, G. H. 1994, ApJ, 433, L9
Smith, P. S., Schmidt, G. D., Allen, R. G., & Angel, J. R. P. 1995, ApJ, 444, 146
Soifer, B. T., Sanders, D. B., Madore, B. F., Neugebauer, G., Danielson, G. E., Elias, J. H., Lonsdale, C. J., & Rice, W. L. 1987, ApJ, 320, 238
Solomon, P. M., Downes, D., & Radford, S. J. E. 1992, ApJ, 387, L55
Thronson, H. A., Jr., & Greenhouse, M. A. 1988, ApJ, 327, 671
Thronson, H. A., Jr., Majewski, S., Descartes, L., & Hereld, M. 1990, ApJ, 364, 456
Tomisaka, K., & Ikeuchi, S. 1988, ApJ, 330, 695
Tonry, J., & Davis, M. 1979, AJ, 84, 1511
Tremaine, S., Richstone, D. O., Byun, Y.-I., Dressler, A., Faber, S. M., Grillmair, C., Kormendy, J., & Lauer, T. R. 1994, AJ, 107, 634
Vacca, W. D., & Conti, P. S. 1992, ApJ, 401, 543
Veilleux, S., Kim, D.-C., Sanders, D. B., Mazzerella, J. M., & Soifer, B. T. 1995, ApJS, 98, 171
Williams, D., Thompson, C. L., Rieke, G. H., & Montgomery, E. F. 1993, Proc. SPIE, 308, 482
Wynn-Williams, C. G., & Becklin, E. E. 1993, ApJ, 412, 535
Wynn-Willams, C. G., Eales, S. A., Becklin, E. E., Hodapp, K.-W., Joseph, R. D., McLean, I. S., Simons, D. A., & Wright, G. S. 1991, ApJ, 377, 426
Zenner, S., & Lenzen, R. 1993, A&AS, 101, 363
Zhou, S., Wynn-Williams, C. G., & Sanders, D. B. 1993, ApJ, 409, 149